Journal of Optoelectronics and Advanced Materials Vol. 7, No. 5, October 2005, p. 2281 - 2291

SULFIDE, SELENIDE AND TELLURIDE GLASSY SYSTEMS FOR OPTOELECTRONIC APPLICATIONS

D. Lezal[a*], J. Zavadil[b], M. Prochazka[c]

[a]Laboratory of Inorganic Materials, Institute of Inorganic Chemistry AS CR, 250 68 Prague-Rez, Czech Republic
[b]Institute of Radio Engineering and Electronics AS CR, 182 51 Prague 8, Chaberska 57, Czech Republic
[c]Rehabilitation Centre Jarov, Prague 3, Konevova 205, Czech Republic

Chalcogenide glasses form very wide family of non–oxide glasses which contain chalcogenide elements in combination with selected elements from III, IV, V, VI group of periodic system. These glasses opposite to SiO_2 ones exhibit transmission in middle and far infrared region of spectra, higher values of refraction index and thus are very promising materials for drawing active and passive optical fibers for use in medicine and sensing. There are very important demands on preparation of base glasses in high chemical and physical purity and on detailed diagnostic measurements of their properties. Physical properties of these glassy systems are strongly influenced by the presence of structural units and chemical bonds and by the presence of one or more glass forming region. The attention in this paper is focused on the preparation of high purity base glasses, their doping with rare earth elements, and on optical and fluorescence measurements, X-ray analysis and fiber drawing.

(Received August 25, 2005; accepted September 22, 2005)

Keywords: Sulfide, Selenide, Telluride glasses, Optical and fluorescence properties, Structural units, Applications

1. Introduction

There is a growing interest in the family of special glasses namely chalcogenide glasses and heavy metal oxide glasses (HMO) due to their promising properties such as the transparency in middle and far infrared regions of spectra, higher values of refraction indices and lower values of phonon energy opposite to SiO_2 or fluoride glasses. These glasses and optical fibers can be used as passive medium for laser power delivery. Generally speaking, these systems can contain one or more chalcogen elements in combination with elements from IIIth, IVth, Vth, VIth or VIIth group of periodic system. These glasses belong to the group of glassy semiconductors having *p*-type conductivity, are characterized by the value of forbidden band $E_g \sim 2$ eV and therefore are transparent in middle and far infrared regions of spectra. Their transparency region is defined by a short wavelength absorption edge, related to the electronic band gap, and by fundamental vibrations of chemical bonds at long wavelengths. Between these two edges, due to intrinsic absorption, could be observed various absorption bands that indicate the presence of impurities (extrinsic absorption).

There are differences between sulfide, selenide and telluride glasses in glass forming region (GFR) and glass forming ability (GFA). These are influenced by the presence of various structural units and by the existence of chemical bonds which are built up in to base glassy skeleton. Interesting changes were observed in systems having two or more GFR, for example Ge-As-Te systems, that have two regions, one rich in $[TeTe_{2/2}]$ structural units and Te–Te bonds, the other rich in $[AsAs_{3/3}]$ units and Te–Te bonds.

* Corresponding author: lezal@iic.cas.cz

The survey of important properties of selected chalcogenide glasses is given in [1,2]. The above mentioned differences between sulfide, selenide and telluride glasses in GFA and GFR are further supplemented by the differences in thermal stability and the position of the edges at short and long wavelengths of the spectra. Generally, it is valid that sulfide and selenide glasses are more stable than telluride ones, which have worse GFA, smaller GFR, lower transmission and higher refraction index and also they have higher tendency to crystallization and phase separation.

It should be noted that both the study and applications demand high chemical and physical purity. To achieve values of suitable optical losses the concentration of hydrides (OH, H_2), oxides and hydrocarbonates must be in the range of 10^{-5}–10^{-6} mol% and the concentration of physical defects in the range 10^2–10^3 cm^{-3}. For this reason new progressive purification and preparation procedures were developed [3,4]. Telluride and mix selenide–telluride glasses are also attractive for active devices due to their low phonon energies and higher values of the refractive index. Thus, doping of these glasses by rare earth (RE) elements and the luminescence efficiency of RE^{3+} ions are being studied extensively [5,6]. The luminescence efficiency of inner shell 4f-4f radiative transitions of RE^{3+} ions turns out to be strongly dependent on the solubility of RE ions in the host glass and on the presence of OH groups. The presence of OH groups supports the rise of clusters and decreases the luminescence efficiency.

In the paper we survey the preparation and properties of selected sulfide, selenide and telluride glass systems both base and doped with RE elements and some aspects of their applications in optoelectronics.

2. Experimental

2.1. Preparation of chalcogenide glasses

Glasses were prepared by direct synthesis from mixture of pure starting elements. For purification of starting elements sublimation, distillation and gettering processes were used. Selected glass systems were doped by RE elements (Pr, Er), with concentrations in the range 500 – 1500 wt. ppm. Details of technological procedure and of special technological setups are given in detail elsewhere [3,4].

2.2. Structure of glasses

The glass forming region (GFR) and glass forming ability (GFA) of selected glass systems will be discussed in more detail. GFR includes all possible combinations of concentrations of elements of a given system that can enter into the glassy state by cooling melts. Areas of GFR vary and depend on glass composition, structural units and chemical bonds. Some systems have one, two or more GFR, for example Ge-As-Te glasses. Generally, is valid that GFR decreases with higher atomic number of chalcogenide elements, from sulfide to telluride glasses. More stable glasses can be found in the middle of GFR and around eutectic alloys. GFA is closely connected with glass forming region the larger the GFR, the better GFA. Structural skelets of prepared glasses are built up from structural units which can be planar [$SS_{2/2}$], trigonal [$AsX_{2/3}$] or tetragonal [$GeX_{4/2}$], where X stands for S, Se, or Te. Chalcogenide glasses can be stoichiometric as $As_{40}X_{60}$, where their valency electrons are fully saturated and only one kind of chemical bonds exists. For example $As_{40}S_{60}$ structural units have only three As-S bonds and in $Ge_{33}Se_{67}$ system, valency requirements lead to the formation of fully saturated [$GeSe_{4/2}$] units with four Ge-Se bonds. When the concentration of Ge or Se is higher than in fully saturated composition, i.e. in Ge_xSe_{100-x} then besides [$GeSe_{4/2}$] structural units there exist also [$SeSe_{2/2}$] or [$GeGe_{4/2}$] ones with Se-Se or Ge-Ge bonds. The concentration of structural units is given by the relation $c[AB_x]=d/M$ where d is density of glass and M molar weight of structural units. The number of covalent bonds v in glasses can be calculated according to the relation $v=z\times c[AB_x]$, where z is the number of covalent bonds in the structural unit and $c[AB_x]$ is the concentration of structural units. The survey of structural units and number of covalent bonds is given in [1,7].

For Ge-As-Te glasses there exist two GFR, the Te- rich and As- rich ones. For this study three compositions were chosen: systems with Te-rich as well as As-rich composition and fully saturated one. In Te–rich glasses, e.g. $Ge_{10}As_{20}Te_{70}$ the following bonds can be found: Te-Te from [$TeTe_{2/2}$] structural units and Ge-Te bonds from [$GeTe_{4/2}$] ones. Similar structure is valid for non-saturated glasses rich in selenides or tellurides components. In the fully saturated composition, such as $Ge_{10}As_{28}Te_{62}$, only Ge-Te and As-Te bonds exist from [GeTe4/2] and [$AsTe_{3/2}$] units which are connected by weak Van der Waals forces. This structural skeleton influences GFA too. GFA of these systems is not as good as that for systems prepared with sulfur or selenium. The poorest GFA was observed at fully saturated glass composition where only [$AsTe_{3/2}$] and [$GeTe_{4/2}$] structural units exist.

For confirmation of these conclusions selected samples were heated to crystallization temperature and results of X-ray analysis measurements were compared with the measurement of unheated glasses.

3. Diagnostic measurements

The composition has been monitored via quantitative Electron Diffraction X-ray (EDX) analysis, the homogeneity of prepared glasses was investigate by microprobe Kevex and oxygen concentration by LECO316 equipment. These measurements show that the difference between theoretical and real values in composition of prepared glasses was less than 6% on average.

Infrared absorption spectra were measured in the visible range on Specord M400 and in NIR by Matson Galaxy 300 (with the spectral range up to 20 μm). The attention was focused on the measurement of absorption edges and on the determination of intrinsic and extrinsic absorption bands.

Structural X-ray analysis was carried out on Siemens D 5005 (Bruker – AXC). By this methods the crystallization phase, structural units and chemical bonds was investigated and it enabled to determine non-crystalline and crystalline phases after temperature annealing at the crystallization temperature.

Differential thermal analysis has been performed by using equipment Netzsch 429 with the heating rate 5 ^{o}C /min in nitrogen atmosphere.

Photoluminescence (PL) spectra were taken at various temperatures and various levels of excitation by He-Ne and Ar ion lasers in an optical He closed cycle cryostat enabling measurements in the temperature range 3.5 – 300 K. The 1 m focal length monochromator with the cooled Edinburgh Instruments Ge detection system or cooled GaAs photo-multiplier enables sensitive and high resolution measurement in the spectral range 400-1700 nm by using the lock-in technique and the computer controlled data collection.

4. Results and discussion

4.1 Sample preparation

Glass rod 9-10 mm in diameter and 100 mm in length have been obtained. Glasses were prepared in special technological setups described in [1,3,4]. The concentration of OH and oxide impurities was calculated from the intensity of the absorption bands at 2.97 μm (OH)**,** 6.35 μm (H_2O), 4.01 μm (H_2S), 4.58 μm (H_2Se) and 6-12 μm (oxides). The average concentrations of impurities were about of 10^{-5} mol% [1,8]. The difference between theoretical and real weight is about 2%.

4.2 Structure of glasses – GFR and GFA

Glasses on the base of sulfide and selenide compounds exhibit wide GFR and very good tendency to form glass solids. They have only one GFR, trigonal and tetragonal structural units, which are connected mostly by chalcogenide bridges. As it was stated above the Ge-As-Te system

has two GFR–Te rich region and As–rich one. The GFR for this system according to Nielson [9] and Tanaka [10] are shown in Fig. 1a and 1b, respectively.

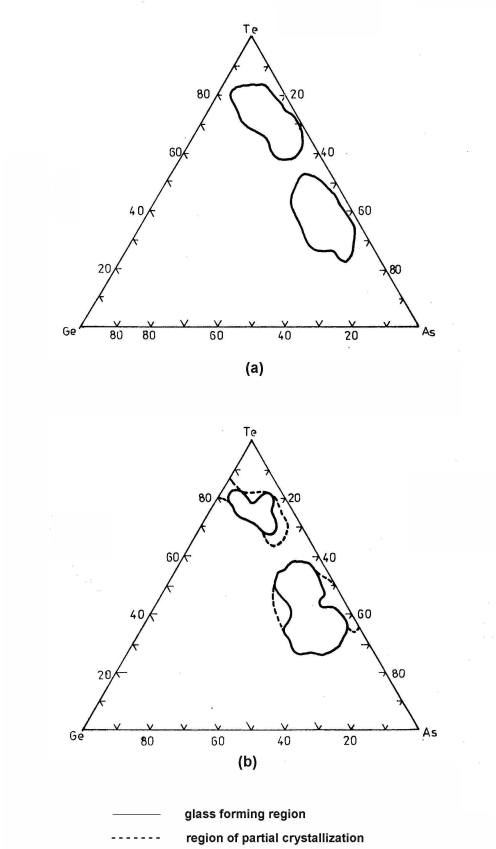

Fig. 1. The glass forming region of the system Ge-As-Te according to Nielson [9] and according to Tanaka [10] are given in parts (a) and (b), respectively. The full line encloses the glass forming region while the dashed line the region of partial crystallization.

In order to confirm the proposed structural model on the base of given structural units and chemical bonds, all compositions of studied glasses were heated to their crystallization temperature and afterwards X-ray analysis was carried out. Results are shown in Fig. 2; 3 and 4. On Fig. 2 there is an angle resolved spectrum of non-crystalline glassy solid and as it can be seen no crystallization peaks were observed.

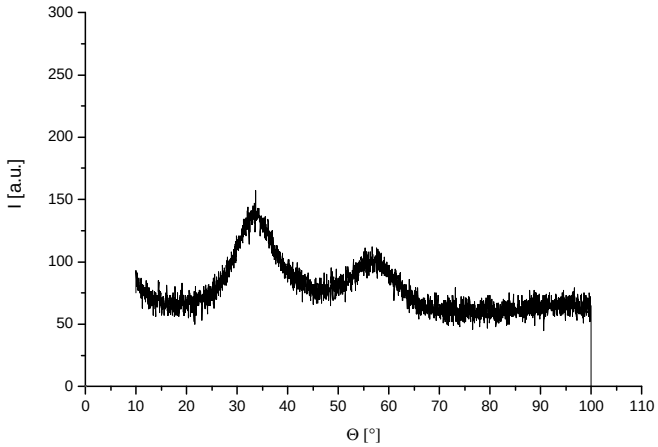

Fig. 2. X-ray diffraction pattern of $Ge_{10}As_{20}Te_{70}$ glass system is shown. The system does not show any crystalline phase.

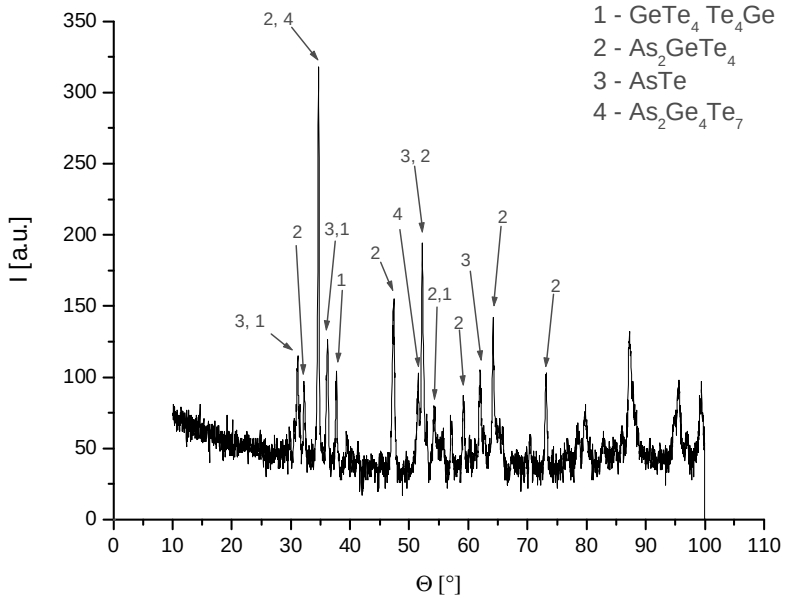

1-$GeTe_4$ Te_4Ge cubical a = 11.0900 Å, 2-As_2GeTe_4 rhombohedral (a = 4.0725 Å), 3-AsTe cubical (a = 5.7780 Å), 4-$As_2Ge_4Te_7$ rhombohedral (a = 4.1060 Å)

Fig. 3. X-ray diffraction pattern spectrum of $Ge_{10}As_{40}Te_{50}$ glass system is shown. The presence of crystalline phase is indicated by arrows and described in the inset.

In As-rich glasses, such as the one shown in Fig. 3, the crystallization peaks of [$AsAs_{3/3}$], [$GeTe_{4/2}$] and [$AsTe_{2/2}$] structural units are present. On the other hand in Te rich glasses crystallization peaks of [$AsTe_{3/2}$], [$GeTe_{4/2}$], [$TeTe_{2/2}$] structural units are observed. X-ray analysis of fully saturated composition, shown in Fig. 4, gives similar results as Te- rich composition. The x-ray diffraction pattern of binary systems $As_{40}Te_{60}$ and $Ge_{15}Te_{85}$, after heating to the crystallization temperature and with well resolved crystallization peaks is shown in Fig. 5.

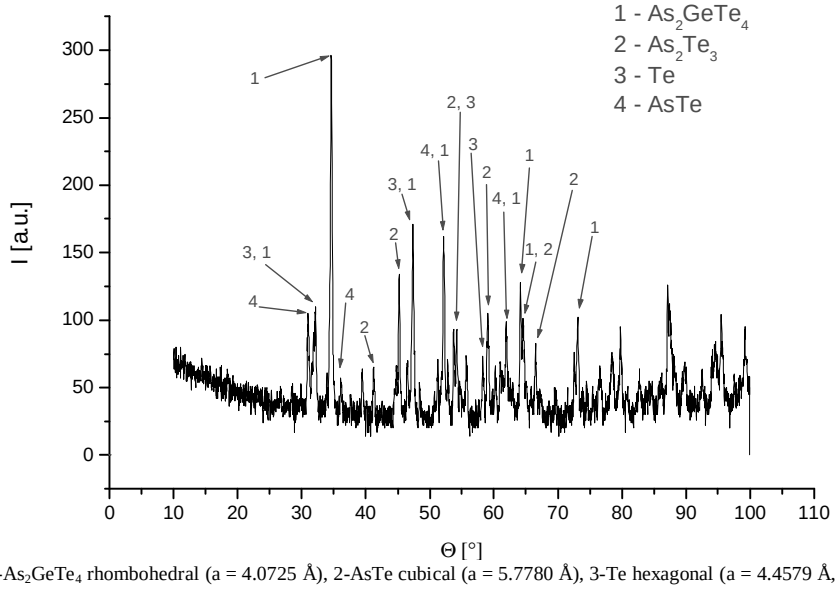

1-As_2GeTe_4 rhombohedral (a = 4.0725 Å), 2-AsTe cubical (a = 5.7780 Å), 3-Te hexagonal (a = 4.4579 Å, c = 5.9270 Å)

Fig. 4. X-ray diffraction pattern of $Ge_{10}As_{28}Te_{62}$ glass system is shown. The presence of crystalline phase is indicated by arrows and described in the inset.

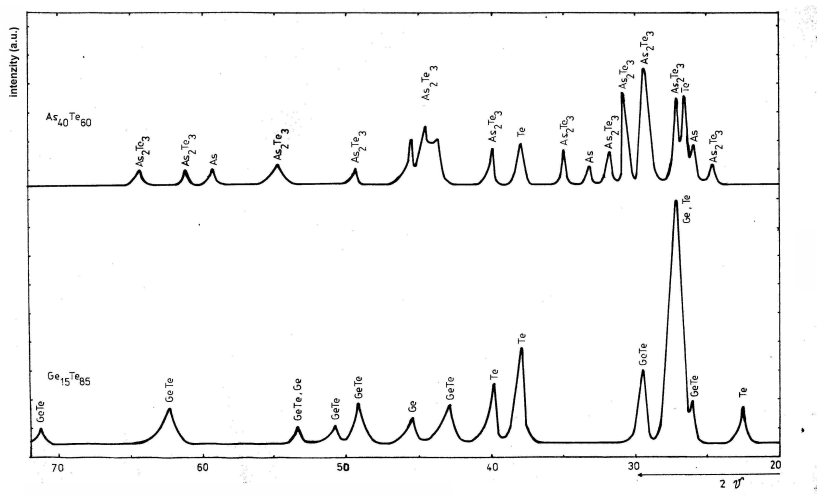

Fig. 5. X-ray diffraction patterns of $As_{40}Te_{60}$ (the upper curve) and $Ge_{15}Te_{85}$ (the lower curve) systems, is shown.

4.3 Optical properties

Infrared absorption spectroscopy was used for the detection of intrinsic and extrinsic absorption bands, the transmission range and refraction index.

1. Sulfide glasses – transparency region is 0.5 – 6 μm, transmission is about 80%, refraction index of about 2.35 and the scattering losses very low. Glass rod was used as a preform for fiber drawing, 250 – 700 μm in a diameter and 150 m in length. These optical fibers are suitable as transport medium of laser power delivery (Er:YAG laser radiation for use in dentistry). Main impurities causing extrinsic absorption are OH and H_2S.
2. Selenide glasses – transparency region is 0.8 – 11 μm, transmission 70%, refractive index of about 2.72. Optical fibers 450 μm in diameter were prepared and could be used as transport medium of power energy of Er:YAG, CO and CO_2 lasers. Main sources of extrinsic absorption are OH, H_2Se, H_20 and C-H impurities.
3. Telluride glasses – the higher attention was paid to these systems. The thickness of measured samples was from 2 up to 40 mm, transmission is about of 58%, refraction index about of 3.40 .The position of the short wavelength absorption edge is shifted towards longer wavelengths due to the presence Te (substitution of S or Se with Te), for the substitution of 30 at.% the position of the absorption edge is 1.25 μm and for 50 at.% Te the position of absorption edge is 1.47 μm. The shift of the absorption shoulder of intrinsic 3 and 4 phonon processes can also be observed. This intrinsic absorption is caused primarily by fundamental and overtone bands of Ge-Se bonds. Further, by replacement of Se by Te atoms new structural units arise and because Te atoms are heavier than Se ones, the shift of intrinsic absorption is observed to longer wavelengths. Typical absorption spectra of $Ge_{20}Se_{80}$ and $Ge_{20}Se_{80-x}Te_x$ glasses are shown in Fig. 6 and 7 for VIS and NIR ranges. It could be seen that the short-wavelength absorption edge is being shifted towards longer wavelength due to the replacement of Se by Te. The absorption band at 4.5 μm is due to Se-H groups. The pronounced absorption band at 12.5 μm observed on two samples (x=8, x=10), and superimposed on absorption band due to Ge-Se bonds, is caused by Ge-O bonds. This absorption band could be diminished or removed when baking of Ge, together with gettering is performed under vacuum prior to the start of the synthesis. At some samples with higher Te concentration the transmission decreases also due to partial crystallization and phase separation. In these cases scattering losses increase. The infrared absorption spectrum of $Ge_{10}As_{40}Te_{50}$ glasses are shown on Fig. 8. On this figure it is possible to observe extrinsic absorption and the positions of extrinsic absorption bands on not purified samples, these absorption bands disappear after purification.
4. The main absorption bands of extrinsic absorption and its positions are given in Table 1.

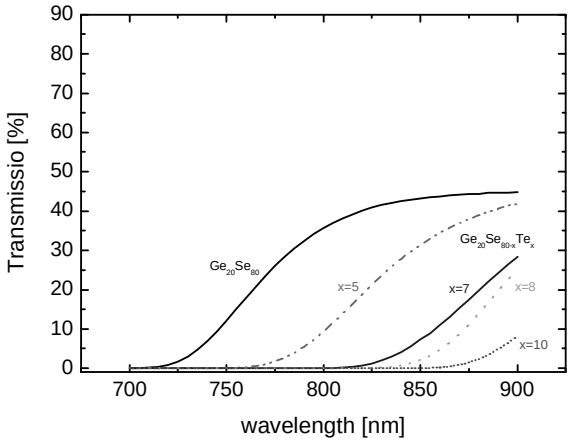

Fig. 6. The comparison of short wavelength edge of $Ge_{20}Se_{80}$ and $Ge_{20}Se_{80-x}Te_x$ glass samples. The values of x=5,7,8,10, are indicated in the figure. The thickness of measured samples was 0.2 cm.

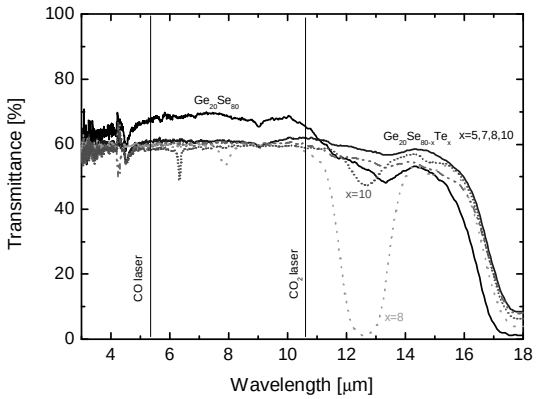

Fig. 7. NIR transmission spectra up to the long wavelength absorption edge are shown for $Ge_{20}Se_{80}$ and $Ge_{20}Se_{80-x}Te_x$ glassy samples. The values of x=5,7,8,10, are indicated in the figure.

Table 1. Absorption bands of extrinsic impurities built in skeleton of As-S, As-Ge-Se and Ge-Se chalcogenide glass systems.

Impurities		Wavelengths (μm)		
		As-S	As-Ge-Se	Ge-Se
OH	Fundamental	2.91	2.92	2,94
	Overtone	1.44	1.45	1.43
	Combination	2.29, 1.92	2.32, 1.92	2.25, 1.88
SH SeH	Fundamental	4.03	4.57	4.00
	Overtone	2.05	2.32	2.02
	Combination	3.69	2.32	6.32
H_2O		6.32. 2.77	6.32, 2.76	6.32, 2.76
C		4.94	4.94	4.94
Oxides			7.0 – 9.0	

4.4. Differential thermal analysis

The differential thermal analysis (DTA) of $Ge_{15}Te_{85}$ and $As_{40}Te_{60}$ systems is shown in Fig. 9 by the upper and lower curve, respectively. The temperatures of glass transition (T_g), that of crystallization (T_x) and of glass melting (T_m) are given for selected systems in Table 2. DTA measurements show that T_g and T_m temperatures decrease and exothermic peak at T_x increases with growing Te concentration.

Table 2. The temperatures of glass transition (T_g), that of crystallization (T_x) and of glass melting (T_m) are shown for selected systems.

Composition	T_g (°C)	T_x (°C)	T_m (°C)
$Ge_{30}Se_{70}$	318	416	476
$Ge_{30}Se_{40}Te_{30}$	262	344	466
$Ge_{30}Se_{20}Te_{50}$	224	336	450
$Ge_{20}Te_{80}$	155	228	360
$Ge_{10}As_{10}Te_{70}$	127	234	379
$As_{40}Te_{60}$	147	273	378

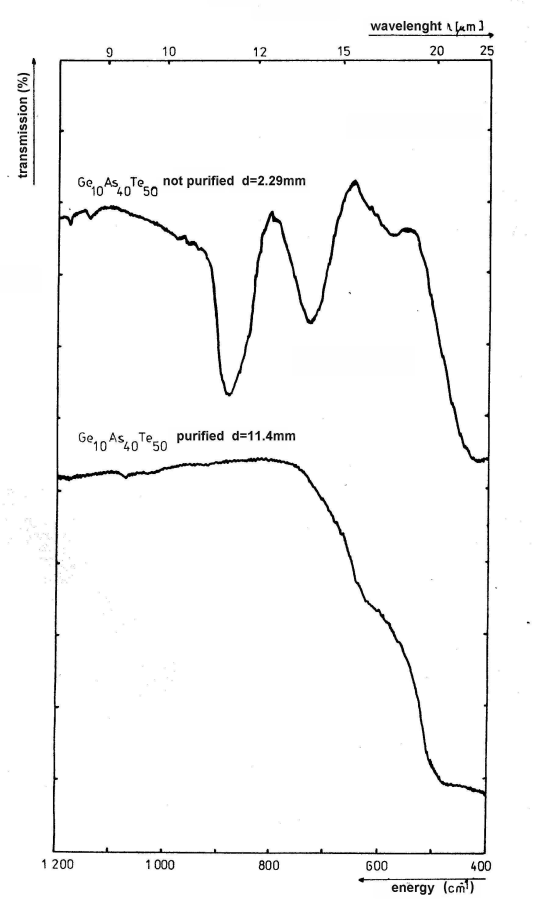

Fig. 8. The infrared part of the transmission spectrum of $Ge_{10}As_{40}Te_{50}$ is shown as a function of energy. As it is indicated in the inset, the upper and the lower curves give the spectra of non-purified and purified samples, respectively.

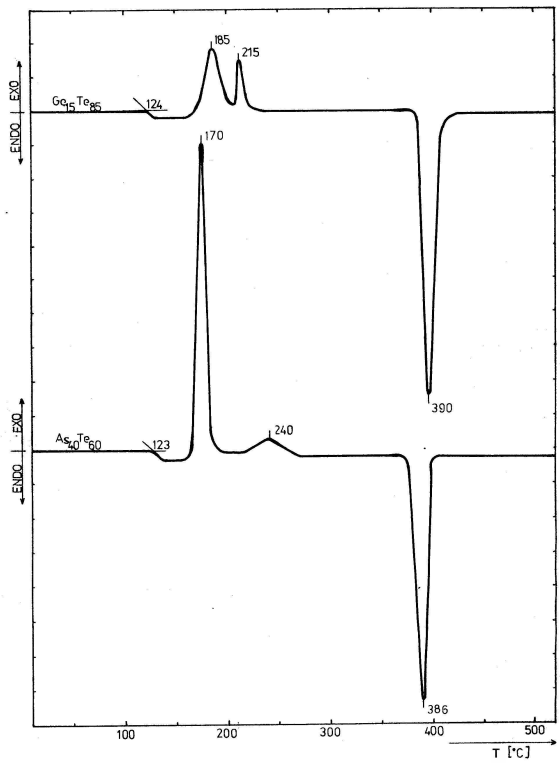

Fig. 9. The differential thermal analysis of samples $Ge_{15}Te_{85}$ and $As_{40}Te_{60}$ is shown by the upper and lower curve, respectively.

4.5 Low-temperature photoluminescence

PL spectra of multi-component alloys $Ge_{20}Se_{80-x}Te_x$ with various amounts of Te have been measured at different temperatures. The influence of substitution of Te for Se on the dominant luminescence band, at about half the band gap energy [11], is demonstrated in Fig. 10, where low temperature PL spectra are shown for x=0, 5, 8 and 10.

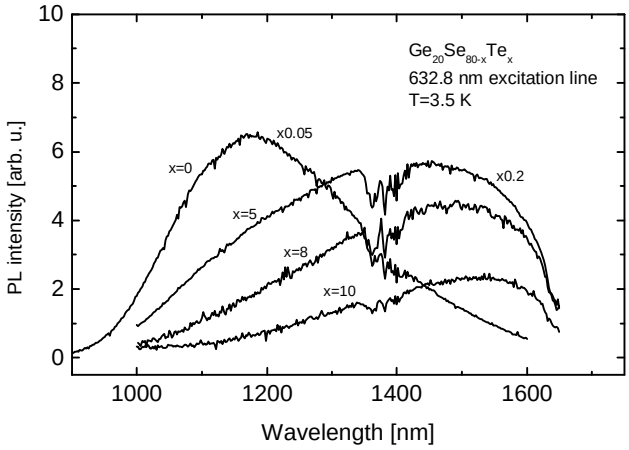

Fig. 10. Low temperature PL spectra of $Ge_{20}Se_{80-x}Te_x$ are shown for x=0, 5, 8 and 10. The substitution of Te for Se significantly shifts the luminescence band to longer wavelengths.

A shift of dominant luminescence band from 1150 nm ($Ge_{20}Se_{80}$) to 1550 nm ($Ge_{20}Se_{70}Te_{10}$) could be seen. The structure at about 1350 nm is due to absorption of emitted luminescence radiation on water vapours in the air. It is seen because there is a strong signal within the water vapours absorption range. Both position and line width of the luminescence band are not strongly temperature dependent up to 200 K. The asymmetry of the spectral shape for higher Te content is due to cut off of Ge detection system beyond 1700 nm. Low temperature base glass luminescence together with sharp transitions due to Er or Pr doping are shown in Fig. 11. PL spectra of $Ge_{20}Se_{80-x}Te_x$, for x=0 and 7, doped with Er and Pr together with the spectrum of $Ge_{20}As_{15}Se_{65}$ doped with Pr are shown by curves (a), (b) and (c), respectively. The peculiar peak at 1590 nm is due to Pr doping but does not correspond to reported 4f-4f inner shell transitions of Pr^{3+} ion in glassy material. We suggest that it corresponds to the the $^1D_2 \rightarrow {}^1G_4$ transition that becomes effective in studied glass system. We have observed identical Pr^{3+} transitions also in the GeAsS doped with 1500 wt. ppm of Pr. Only one 4f-4f transition of Er^{3+} was clearly seen on all measured samples as shown in curve (a), namely the one corresponding to dominant Er^{3+} transition at 1539 nm.

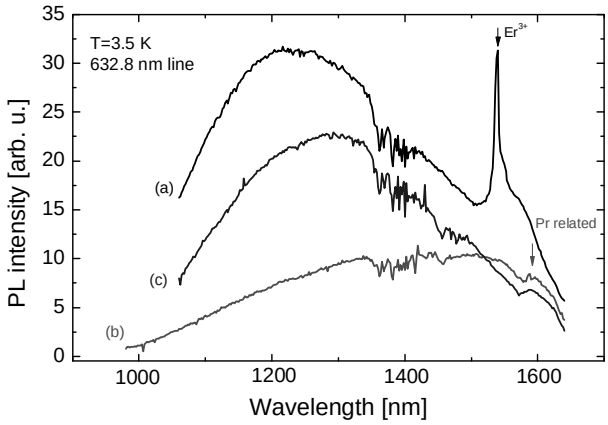

Fig. 11. Low-temperature PL spectra of GeSeTe and GeAsSe glasses are shown. The curves (a), (b) and (c) correspond to $Ge_{20}Se_{80}$:Er, $Ge_{20}Se_{73}Te_7$:Pr and $Ge_{20}As_{15}Se_{65}$:Pr, respectively. The sharp $^4I_{13/2} \rightarrow {}^4I_{15/2}$ transition of Er^{3+} ion at 1539 is seen together with much weaker peculiar peak at 1590 nm due to Pr doping.

4.6 Fiber drawing

In the case of As_2S_3 and As_2Se_3 and their derived components optical fibers were drawn by using rod-tube methods [1,12] or from crucible. The diameter of core of fibers was 300 –550 μm, cladding was from glass or plastic and the numeric aperture 0.2 –O.6.

Telluride optical fibers were drawn from crucible in nitrogen atmosphere with numeric aperture 0.23 – 0.5 [13,14]

Optical fibers are being used in sensing and medical applications. For example in surgery for laser power delivery (Nd:YAG, Er:YAG, CO and CO_2 lasers), for measurements of the tissue temperature or in a form of bundles for infrared imaging.

5. Conclusions

Special technology has been developed for the preparation of pure glasses with considerably reduced concentrations of chemical impurities and physical defects. From among the discussed systems selenide-telluride glasses show less thermal stability and phase separation can be observed at higher Te concentrations. The rise of clusters depends on OH group and RE concentration. Optimum RE concentration falls in the range 500 – 1500 wt.ppm and that of OH group below

5×10^{-5} mol%.

Glass forming regions of selected systems have been discussed in terms of structural units and chemical bonds. Angle resolved rtg analysis of glass systems measured at room temperature and that elevated to the crystallization one has been used to demonstrate the role of structural units. Measurements of transmission spectra enable a quick assessment of basic properties and composition of glass systems. Short wavelength absorption edge shifts towards longer wavelength as a result of Te → Se substitution.

The dominant feature of luminescence spectra of studied glass systems is a broad band centred at about half the band-gap energy. Both peak position and the line width increase with the band-gap energy. Particularly, the substitution of Te for Se results in the shift of low-temperature luminescence band to lower energy reflecting the lower band gap of GeSeTe system. All systems doped with Er exhibit a strong luminescence due to $^4I_{13/2}\rightarrow{}^4I_{15/2}$ transition of Er^{3+} ion at 1539 nm. However, we did not observe the $^1G_4\rightarrow{}^3H_5$ transition of Pr^{3+} ion. Instead we observed, on all Pr doped samples, a relatively weak luminescence peak at 1590 nm, which we tentatively assign to distorted $^1D_2\rightarrow{}^1G_4$ transition of Pr^{3+} ion.

Prepared glasses and corresponding optical fibers [15] could be used as biosensors and in medicine as transmission medium for power lasers, for autofluorescence spectroscopy of cancerous tissue or for measurements of tissue temperature.

Acknowledgment

This work has been supported by the Grant Agency of the Czech Republic, grant no. 104/05/0878.

References

[1] D. Lezal, P. Macko, Non-Crystalline Semiconductors, ALFA, Bratislava,1988.
[2] M. A. Popescu, Non-Crystalline Chalcogenides, Kluwer Academic Publisher, Dordrecht/Boston/London, 2000.
[3] D. Lezal, J. Optoelectron. Adv. Mater. **5**(1), 23 (2003).
[4] D. Lezal, L. Pedlikova, M.Poulain, Proc. SPIE 3416, Quebec, Canada, 1993, p.43.
[5] A. Zakery, S. R. Elliott, J. of Non-Crystalline Solids **330**, 1 (2003).
[6] J. Heo, J. of Non-Crystalline Solids **326&327**, 410 (2003).
[7] J. L. Mjuler, Chemistry of the Solid State, Technical publishing, Leningrad 1978 (in Russian).
[8] D. Lezal, J. Pedlikova, J. Zavadil, J. Optoelectron. Adv. Mater. **6**(1) 133 (2004).
[9] S. Nielson, Infrared Physics **5**, 195 (1965).
[10] K. Tanaka, J. of Non-Crystalline Solids **12**, 10 (1970).
[11] B. T. Kolomiets, T. N. Mamontova, A. A. Babaev, J. of Non-Crystalline. Solids **4**, 289 (1972a).
[12] J. Kobelke, J. Kirchhof, M. Scheffer, IFPH, Research report, Jena, 1997.
[13] D. M. Rusconi, G. H. Siegel, Proc. Infrared Optics Materials, Vol. **929**, 1988.
[14] T. Arai, Makoda Kikuchim J. Appl. Phys. **63**(9), 1 (1988).
[15] X. Zhang, H. Ma, J. Lucas, J. Optoelectron. Adv. Mater. **5**(5), 1327 (2003).